Excitation mechanism of low-n edge harmonic oscillations in ELM-free high performance tokamak plasmas

D. Brunetti,[1,*] J. P. Graves,[2] E. Lazzaro,[1] A. Mariani,[1] S. Nowak,[1] W. A. Cooper,[2] and C. Wahlberg[3]

[1]Istituto di Fisica del Plasma IFP-CNR, Via R. Cozzi 53, 20125 Milano, Italy
[2]École Polytechnique Fédérale de Lausanne (EPFL), Swiss Plasma Center (SPC), CH-1015 Lausanne, Switzerland
[3]Department of Physics and Astronomy, P.O. Box 516, Uppsala University, SE-751 20 Uppsala, Sweden

(Dated: March 27, 2019)

The excitation mechanism for low-n Edge Harmonic Oscillations in quiescent H-mode regimes is identified analytically. We show that the combined effect of diamagnetic and poloidal MHD flows, with the constraint of a Doppler-like effect of the ion flow, leads to the stabilisation of short wavelength modes, allowing low-n perturbation to grow. The analysis, performed in tokamak toroidal geometry, includes the effects of large edge pressure gradients, associated with the local flattening of the safety factor and diamagnetic flows, sheared parallel and $\boldsymbol{E}\times\boldsymbol{B}$ rotation and a vacuum region between plasma and the ideal metallic wall. The separatrix also is modelled analytically.

Introduction.— Tokamak high-confinement (H-mode) regimes are attractive operating scenarios for fusion reactors because of their long energy confinement time [1]. The large edge pressure gradients, which characterise H-mode plasmas, favour the formation of short wavelength magnetohydrodynamic (MHD) perturbations called edge localised modes (ELMs) [2]. Rapid energy and particle expulsions are usually associated with ELMs. Though this can be beneficial for impurity control, ELMs deposit unacceptable peak heat loads on the divertor target causing a severe deterioration of the plasma facing components. This motivates a lively line of research focussed on the development of sustained high confinement regimes with intrinsically no ELMs.

One of the most promising high performance naturally ELM-free operating regimes is the so called quiescent high-confinement (QH) mode [3–5]. QH scenarios are usually observed at low edge collisionality ($\nu_e^* < 0.3$) over a fairly broad range in q_{95} ($3 \lesssim q_{95} \lesssim 6$) [6, 7]. At low ν_e^*, large edge pressure gradients are associated with a significant bootstrap contribution to the current. In QH plasmas ELMs are suppressed and replaced by low-n steady mild MHD perturbations called edge harmonic oscillations (EHOs). These have been observed in DIII-D [4, 6–8], ASDEX-U [5, 9], JET [10], and JT-60U [11]. The edge particle transport is enhanced by EHOs, thus allowing density control and potentially ash removal without the impulsive heat load problem [6, 12]. EHOs are dominantly low-n perturbations (usually $n \sim 1, 2$) accompanied by weaker higher-n modes up to $n \sim 10$ [5, 7, 8]. A single EHO harmonic n rotates with frequency $n\Omega_{ped}$ (Ω_{ped} is the plasma toroidal rotation frequency at the pedestal top) [3, 10, 13].

The excitation mechanism of such instabilities is still unclear. Previous theoretical interpretations suggested that short wavelength modes exhibiting *infernal* features [13–16], though dominant in the linear phase, were suppressed nonlinearly and superseded by steady low-n modes [17, 18] with no significant effects of the parallel flow [17, 19]. Recent experimental findings point to the $\boldsymbol{E}\times\boldsymbol{B}$ shearing rate as the key ingredient for the development of the characteristics of these oscillations [19]. Indeed numerical investigations of QH-mode DIII-D plasma discharges with sheared $\boldsymbol{E}\times\boldsymbol{B}$ flows showed that low-n modes are linearly dominant and are eventually sustained in the nonlinear stage at moderately low amplitude [7, 20–24].

In this Letter the specific physical mechanisms which allow low-n EHOs to emerge are identified by extending the analysis of Ref. [25] within the *infernal model* framework. Features of both external kink and infernal modes are required, viz. vacuum between plasma and wall (*external kink*) and a region of large pressure gradient and low magnetic shear (*infernal*). Our new analytic work, focusses on the linear stability of moderately low-n ideal external-infernal (*exfernal*) modes with the inclusion of toroidal effects and toroidal and poloidal flows (both MHD and diamagnetic). It shows that short wavelength modes are entirely suppressed. Hence the linear calculations show that ELM free H-mode regimes are established by robustly preventing infinitesimally small amplitude short wavelength modes.

Physical model.— Let us analyse small inverse aspect ratio tokamak geometry ($\varepsilon = a/R_0 \ll 1$ where R_0 and a are the major and minor radii respectively), with shifted circular toroidal surfaces. We consider a low-$\beta = 2\mu_0 p/B_{ax}^2 (\sim \varepsilon^2)$ plasma, where p is the pressure and B_{ax} the magnetic field strength on the axis. A right handed straight field line coordinate system (r, ϑ, φ) is introduced where r is a flux label with the dimensions of length, ϑ (counter-clockwise in the poloidal plane) and φ are the poloidal-like and toroidal angles respectively with contravariant basis vectors $(\boldsymbol{\nabla} r, \boldsymbol{\nabla}\vartheta, \boldsymbol{\nabla}\varphi)$. We assume that additional effects (i.e. non-static or beyond MHD, e.g diamagnetic) do not alter to leading order of the standard static equilibrium (whose associated metric tensor coefficients can be found in Ref. [26]). The equilibrium magnetic field in the plasma is $\boldsymbol{B} = T\boldsymbol{\nabla}\varphi - \boldsymbol{\nabla}\psi \times \boldsymbol{\nabla}\varphi$ where ψ is the poloidal flux.

The plasma is described by the ideal drift-MHD equa-

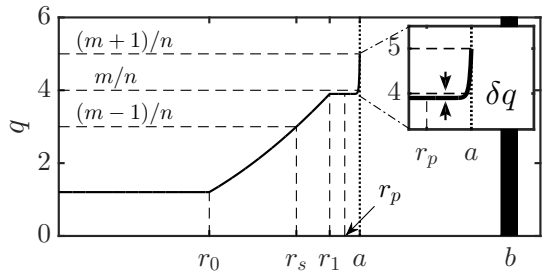

Figure 1. Example of a model safety factor profile employed in our analysis. Note the $(m+1)/n$ resonance at the plasma boundary mimicking the separatrix.

tions [27]:

$$\rho\,(d_t \boldsymbol{v} + \boldsymbol{v}^* \cdot \boldsymbol{\nabla} \boldsymbol{v}_\perp) = -\boldsymbol{\nabla} p + \boldsymbol{J} \times \boldsymbol{B}, \tag{1}$$

$$\partial_t \boldsymbol{B} = \boldsymbol{\nabla} \times (\boldsymbol{v} \times \boldsymbol{B}), \tag{2}$$

$$\partial_t p + \boldsymbol{v} \cdot \boldsymbol{\nabla} p + \Gamma p \boldsymbol{\nabla} \cdot \boldsymbol{v}_i = 0, \quad \partial_t \rho + \boldsymbol{\nabla} \cdot (\rho \boldsymbol{v}_i) = 0, \tag{3}$$

where $d_t = \partial_t + \boldsymbol{v} \cdot \boldsymbol{\nabla}$, $\boldsymbol{v}$ and $\boldsymbol{v}^* = m_i \boldsymbol{B} \times \boldsymbol{\nabla} p / (e\rho B^2)$ (m_i is the ion mass) are the plasma MHD and ion diamagnetic velocities respectively with $\boldsymbol{v}_i = \boldsymbol{v} + \boldsymbol{v}^*$, ρ is mass density, $\boldsymbol{J} = \boldsymbol{\nabla} \times \boldsymbol{B}$ the current density (having normalised $\mu_0 = 1$), p the pressure and $\Gamma = 5/3$ is the adiabatic index. The symbol $\perp$ indicates the vector perpendicular projection to the magnetic field, i.e. $\boldsymbol{v}_\perp = \boldsymbol{B} \times (\boldsymbol{v} \times \boldsymbol{B})/B^2$. The Faraday-Ohm's law has been approximated within the limit of nearly isobaric surfaces and small plasma compressibility.

In choosing the equation for the pressure evolution, it has been implicitly assumed that T_i significantly exceeds T_e so that $p_0 \approx p_{0i}$. Moreover, by assuming that T_e is proportional to ρ at equilibrium and that the perturbations of the mass density and the electron temperature are dominated mainly by convection (i.e. the $\boldsymbol{v} \cdot \boldsymbol{\nabla}$ term), we obtain that the perturbed pressure is given by the ion contribution.

The rotational transform profile (denoted with μ with $q = 1/\mu$) is piecewise continuous [25], constant for $0 < r < r_0$ and $r_1 < r < r_p$ ($r_p = (r_1 + a)/2$), with values μ_{ax} and μ_1 respectively ($\mu_{ax} > \mu_1 = 1/(m/n - \delta q)$), while $\mu = \mu_1 (r_1/r)^2$ for $r_0 < r < r_1$. The separatrix is modelled by imposing for $r_p < r < a$ a narrow region of high magnetic shear :

$$(m+1)\mu - n = S\,[1 - (r/a)^\lambda], \quad \lambda \to \infty, \tag{4}$$

where S is a constant such that $\mu(r_p) = \mu(r_1)$ (note that for $\lambda \to \infty$ this high shear region becomes infinitesimally narrow so that we regard the region $r_1 < r < a$ as shear-free). A *vacuum region* between plasma and the ideally conducting wall extends from $r = a$ to $r = b$ (the wall thickness is irrelevant). We refer to the regions $0 < r < r_1$ and $a < r < b$ as the *outer regions*, while the region $r_1 < r < a$ is the *pedestal region* (the q profile and the relevant radial positions are shown in Fig. 1).

An equilibrium helical MHD flow ($v_0^r = 0$, $v_0^\vartheta = \omega_\vartheta(r)$ and $v_0^\varphi = \Omega(r)$ [29]) is assumed. We stress that ω_ϑ is of $\boldsymbol{E} \times \boldsymbol{B}$ origin. Such a flow is sufficiently weak so that the centrifugal corrections to equilibrium pressure and mass density profiles [30] are negligible within the approximations employed in this work [15]. Equilibrium flow and mass density (pressure) gradients are localised within the *pedestal region*. Equilibrium quantities are denoted by the subscript 0 while perturbed ones, denoted by a tilde, have a time dependence of the type $e^{\gamma t}$ (γ complex).

Eigenmode equations.— The *infernal* model [31, 32] assumes the presence of three poloidal Fourier harmonics, one dominant (m) coupled to two neighbouring sidebands ($m \pm 1$). Hence we write the perturbed velocity as $\tilde{\boldsymbol{v}} = \tilde{\boldsymbol{v}}_m(r) e^{i[m\vartheta - n\varphi]} + \sum_{m'=\pm 1} \tilde{\boldsymbol{v}}_{m+m'}(r) e^{i[(m+m')\vartheta - n\varphi]}$ with $\tilde{\boldsymbol{v}}_{m\pm1} \sim \varepsilon \tilde{\boldsymbol{v}}_m$ (since n is fixed, we omit to specify the toroidal mode number in writing the Fourier components). Mode coupling, induced by the metric oscillation of the Jacobian, is favoured in presence of large pressure gradients and field line bending weakening (i.e. weak shear).

In the *inner* and *outer* regions, because of field line bending dominating over inertia and vanishing pressure gradients, different poloidal Fourier harmonics behave independently according to [25, 33] (here $\ell = m, m \pm 1$ and $' \equiv d/dr$):

$$\left[r^3 (\ell\mu - n)^2 \xi_\ell'\right]' - r(\ell^2 - 1)(\ell\mu - n)^2 \xi_\ell = 0, \tag{5}$$

having introduced the Lagrangian-like radial fluid displacement $\xi_\ell = \tilde{v}_\ell^r / \gamma_\ell$ with $\gamma_\ell = \gamma + i\ell\omega_\vartheta - in\Omega$ [34].

The main difficulty is to derive the eigenmode equation for the mth harmonic, which contains the inertial contributions due to $\boldsymbol{E} \times \boldsymbol{B}$ and diamagnetic flows. In the pedestal region we impose the ordering $\delta q/q \sim \varepsilon$ and $\gamma/m \sim \Omega \sim \omega_\vartheta \sim \omega^* \sim \varepsilon\omega_A$ where $\omega^*(r) = \boldsymbol{v}_0^* \cdot \boldsymbol{\nabla}\vartheta$ and $\omega_A = B_{ax}/(R_0\sqrt{\rho_0})$ (the Alfvén frequency with B_{ax} the magnetic field equilibrium value on the axis). To leading order the $\frac{1}{R^2}\boldsymbol{\nabla}\varphi$ projection of (1) yields $\tilde{B}^\varphi = 0$. From the contravariant radial, poloidal and toroidal projections of (2) we obtain respectively $(\sqrt{g}\tilde{B}^r)_\ell = ir(\ell\mu - n)\xi_\ell$, $\frac{1}{r}(r\tilde{v}_m^r)' + im\tilde{v}_m^\vartheta - in\tilde{v}_m^\varphi = 0$ and $\tilde{v}_m^\varphi + \Omega'\xi_m = 0$. It follows that $(\sqrt{g}\tilde{B}^\vartheta)_m = -\frac{1}{im}(\sqrt{g}\tilde{B}^r)'_m$ and $\tilde{B}_m^i \sim \tilde{B}_{m\pm1}^i$. We point out that in case of large radial gradients and poloidal wave numbers the relations above still hold. The perturbed pressure is written in terms of ξ according to $\tilde{p}_\ell = -p_0'\xi_\ell + \delta p_\ell$, where δp is the *non-convective* contribution. In the limit $T_i \approx const$ with δp small, we have $\tilde{\boldsymbol{v}}^* \simeq \frac{\boldsymbol{\nabla}\varphi}{eB_0^\varphi} \times \boldsymbol{\nabla}\left(\frac{\tilde{p}}{n_0}\right)$ (n_0 is the equilibrium numerical density). We take large radial gradients localised within the narrow pedestal region:

$$r d\ln f/dr \gg 1, \quad f = \xi_\ell, \rho_0, p_0, \Omega, \omega_\vartheta.$$

In addition we assume $m \gg 1$ (and so $n = m/q$ with $q \sim 1$).

The equation for the generic radial displacement ξ_ℓ is obtained by applying the operator $\mathbf{D} = \sqrt{g}\boldsymbol{\nabla}\varphi \cdot \boldsymbol{\nabla} \times 1/B_0^\varphi$ on the perturbed momentum equation [35, 36], and then selecting the ℓth Fourier component. Field line bending dominates over inertia in the sidebands equations (modes with poloidal mode number $m \pm 1$), so that additional flow effects play no role in their corresponding eigenmode equations which read [25]:

$$\left(r^{2\pm m}\xi_{m\pm1}\right)' = r^{1\pm2m} L_\pm + \tfrac{1\pm m}{2}\alpha r^{1\pm m}\xi_m, \tag{6}$$

where $L_\pm$ are constants of integration which are determined later. The equation for ξ_m is given by the mth harmonic of the action of $\mathbf{D}$ on (1). At leading order a rather lengthy but straightforward algebra gives (the cylindrical limit proves to be sufficient):

$$\left[\mathbf{D}[\rho\,(d_t \boldsymbol{v} + \boldsymbol{v}^* \cdot \boldsymbol{\nabla} \boldsymbol{v}_\perp)]\right]_m = \frac{i}{mR_0}\left[r^2\,(K\xi_m')' - m^2 K \xi_m\right],$$

with $K = (\gamma_D + im\omega_\vartheta)[\gamma_D + im(\omega^* + \omega_\vartheta)]/\omega_A^2$ and $\gamma_D = \gamma - in\Omega$ having normalised $B_{ax} = 1$. Let us call $Z(\xi_m)$ the rhs of the equation above. In the incompressible limit $\boldsymbol{\nabla} \cdot \tilde{\boldsymbol{v}}_i \to 0$ and $\Gamma \to \infty$ [36–39], assuming $\boldsymbol{\nabla} \cdot \boldsymbol{v}_{i0}$ negligible and writing $\delta p_{m\pm1}$ from the perturbed $\boldsymbol{B}/|\boldsymbol{B}_0|^2$ projection of Eq. (1), we eventually get $[\mathbf{D}(\boldsymbol{\nabla}\delta p)]_m = 2q^2 Z(\xi_m)$, which embodies the Glasser-Greene-Johnson inertia enhancement factor [40]. In deriving the equation above, we assumed $\omega_\vartheta + \omega^* \approx \omega_I$ where ω_I has weak radial gradients [41]. Finally, with $(\delta q/q)a\frac{d}{dr} \sim 1$ and $-2R_0 p_0' q^2 = \alpha \sim 1$ by taking into account only the leading order of $\tilde{B}_{\varphi m}$ and the incompressible part of $\tilde{p}_m$, the action of $\mathbf{D}$ on the rhs of (1) yields the analogous of the lhs of equation (16) in Ref. [31], computed in the above mentioned limit of steep radial gradients and large m. Thus collating these results together and eliminating the sideband displacements $\xi_{m\pm1}$ by means of (6), the eigenmode equation for the main harmonic ξ_m in the *pedestal region* finally reads [25, 31]:

$$r^2\,(Q\xi_m')' - m^2 Q \xi_m + \tfrac{\alpha}{2}\sum \tfrac{r^{\pm m} L_\pm}{1 \pm m} = 0, \tag{7}$$

where $Q = (1+2q^2)K/n^2 + (\delta q/q)^2$. Equations (5), (6) and (7) form the basis for our analysis.

Dispersion relation.— We assume that the profiles of equilibrium mass density, pressure and toroidal rotation are step-like [25], i.e. $f(r)/f(r_1) \sim \theta(r_p - r)$ with $f = p_0, \rho_0, \Omega$ where $\theta(x)$ is the Heaviside step function of argument x. Without loss of generality (with $\omega^* \propto p_0' \sim \delta(r - r_p)$), we choose ω_ϑ of the form [42]:

$$\omega_\vartheta(r) = \omega_E r_p \delta(r - r_p)\Delta + \omega_I,$$

with $\Delta = (a - r_1)/r_p$ and ω_E constant where δ is the Dirac delta. Note that $\int_{r_1}^{a} \omega_\vartheta dr / \int_{r_1}^{a} dr = \omega_E + \omega_I$ where ω_I has a weak radial dependence.

Writing symbolically (7) as $(Q\xi_m')' + f(r) = 0$ we define $F(r) = \int_{r_1}^{r} f(\hat{r})d\hat{r}$ so that $Q\xi_m' + F(r) = C$ where C is a constant of integration. The function F is bounded, thus dividing the previous result by Q (supposed non-vanishing) and then integrating across r_p shows that ξ_m is continuous at r_p. The solutions of Eq. (5) in the region $0 < r < r_1$ and $a < r < b$ for the dominant mode ξ_m provide the appropriate boundary conditions at r_1 and a, namely $\xi_m(r_1) = \xi_m(a) = 0$ [25, 43]. Thus using the profiles for mass density, pressure, toroidal and poloidal MHD flows and solving (7) on the left and on the right of r_p with the boundary conditions at r_1 and a given above, we obtain to leading order:

$$\xi_m \propto \frac{e^{mr/r_p} - e^{m(2r_f/r_p - r/r_p)}}{e^m - e^{m(2r_f/r_p - 1)}}$$

with $r_f = r_1$ for $r < r_p$ and $r_f = a$ for $r > r_p$ where the slowly varying terms in r have been approximated by setting $r \approx r_p$. Note that ξ_m is symmetric about r_p.

To determine the last term on the lhs of (7), first equation (6) is evaluated at r_1 and a providing respectively $\xi_{m\pm1}(r_1)$ and $\xi_{m\pm1}(a)$ (both functions of $L_\pm$). Then, plugging these expressions into Eq. (6) and integrating from r_1 to a gives $\frac{r_p^{\pm m} L_\pm}{1 \pm m} = \xi_m(r_p)\frac{\beta_1 q^2}{\varepsilon_p}\Lambda^{(\pm)}$, where $\beta_1 = 2p_0(r_1)$, $\varepsilon_p = r_p/R_0$ and $\Lambda^{(\pm)}$ are given by Eq. (16) in Ref. [25] whose sideband dependence is embedded in the coefficients $\mathbb{C}_\pm \equiv [rd(\ln \xi_{m\pm1})/dr]_{r_1}$ and $\mathbb{B}_\pm \equiv [rd(\ln \xi_{m\pm1})/dr]_a$.

The quantities $\mathbb{C}_\pm$ are obtained by solving Eq. (5) in the region $0 < r < r_1$ and thus imposing smooth matching of the sideband eigenfunctions $\xi_{m\pm1}$ across r_1 [25, 32]. The constant $\mathbb{B}_-$ is evaluated similarly (the vacuum perturbation obeys (5) as well) with the replacement $r_1 \to a$. These have been computed in Ref. [25] and for large m and small δq they read $\mathbb{C}_+ \approx 3m + 2$, $\mathbb{C}_- \approx m/6 - 1/4$ and $\mathbb{B}_- \approx 2 - 3m$ (in the latter expression we approximated $(a/b)^{2m-2} \to 0$).

Finally $\mathbb{B}_+$ is obtained by solving equation (5) (which is equivalent to (6) for μ constant and $\alpha \to 0$) for $r_p < r < a$ with μ given by (4). The solution for ξ_{m+1} can be expressed exactly in terms of the hypergeometric functions [26], so that forcing ξ_{m+1} to be finite at its own resonant surface and taking the limit $\lambda \to \infty$ yields:

$$\xi_{m+1} \propto (r/a)^{-m-2} + (1 + {}^2/_m)(r/a)^m,$$

from which $\mathbb{B}_+ = 0$. We point out that with an ideally conducting metallic wall directly interfaced with the plasma (i.e. $\mathbb{B}_\pm \to \infty$) the driving term $\Lambda^{(+)} + \Lambda^{(-)}$ is negative implying stability, reflecting the necessary condition of good plasma-wall detachment as observed in various machines [4, 5, 11]. Thus in the limit of large m and sufficiently far wall we may approximate $\Lambda^{(+)} = \frac{m(r_p/a)^{2m}}{1+1/2(r_1/a)^{2m}}$ and $\Lambda^{(-)} = \frac{2m(a/r_p)^{2m}}{1+3(a/r_1)^{2m}}$. The m upper boundary for which the approximations hold can be estimated by requiring $\frac{1}{m} rd \ln \xi_m r/dr|_{r_p} \gtrsim 1$ (for the parameters which will be employed in the numerical evaluation of the growth rate we would take $m \sim 40 - 50$).

Therefore by taking $\gamma_D = \gamma - in\Omega_1$ with $\Omega_1 = \Omega(r_1)$, according to Refs. [25, 30] integration of (7) across r_p yields the dispersion relation which in the limit $q \gg 1$ reads:

$$\frac{\gamma}{n\omega_A} \approx i\left[\frac{\Omega_1}{\omega_A} - q\left(\frac{\omega_I}{\omega_A} + \frac{m^2\omega_E\Delta}{2\mathfrak{D}\omega_A}\right)\right] + \sqrt{\frac{(\beta_1 q)^2\Lambda}{4\mathfrak{D}\varepsilon_p^2} - \frac{\delta q^2}{q^4} - \left(\frac{m^2 q\omega_E\Delta}{2\mathfrak{D}\omega_A}\right)^2} \tag{8}$$

where $\Lambda = \Lambda^{(+)} + \Lambda^{(-)}$ and $\mathfrak{D} = m\coth[m(1 - r_1/r_p)]$ $= (rd\ln\xi_m/dr|_{r_p-\delta}$ with $\delta \to 0$). Hereafter it is understood that ω_A is the value of the Alfvén frequency on the magnetic axis.

By setting $\omega_E = \omega_I = 0$ we recover the dispersion relation derived in [25] (note that the only effect of toroidal rotation is to Doppler shift the eigenmode frequency in agreement

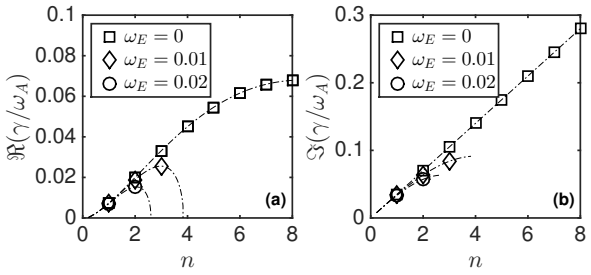

Figure 2. Real (a) and imaginary (b) parts of γ evaluated from Eq. (8) with $q \approx 5$, $\varepsilon = 1/3$, $r_1/a = 0.95$, $\Omega_1/\omega_A = 5 \times 10^{-2}$, $\omega_I/\omega_A = 3 \times 10^{-3}$, $\beta_1 = 0.3\%$ and $\delta q = 0.1$.

with the requirement that EHOs exist with either sign of the toroidal rotation frequency [44]). Indeed the first two terms under the sign of square root are the linear growth rate of the purely MHD perturbation. The imbalance in the inertial contribution of the Doppler correction to γ due to the combination of poloidal MHD and diamagnetic flows, produces the last term in the square root of (8). This term, although small for small m values, increases its amplitude with the poloidal (or equivalently the toroidal) mode number. Hence due to its interplay with the pressure ($\propto \beta$) and field line bending weakening ($\propto \delta q$) driving terms, allows the suppression of short wavelength perturbations favouring the growth of low n modes. This is shown in figure 2 where the real and imaginary parts of γ are computed by means of (8) with reactor relevant parameters. Note that being ω_E different in different machines/regimes, a different number of harmonics can be excited [5, 8]. The $\boldsymbol{E} \times \boldsymbol{B}$ shearing rate estimated as $\omega_E/\Delta \sim \omega_A$ (order of MHz) is in line with the results of Ref. [45]. Finally we point out that the ω_E stabilisation mechanism is independent of mode coupling. Hence it may be expected that if a larger number of coupled harmonics is allowed, with the growth rate driving contribution increasing linearly with n [7, 20], such a stabilisation stills occurs. If additional Doppler contributions enter the diamagnetic flow, stabilisation is nevertheless achieved with the ω_E term in (8) being dominant for short wavelength modes.

Conclusions.— In this Letter the excitation mechanism for low-n EHOs has been identified analytically. Besides the edge local flattening of the safety factor and local sharp pressure gradients [25], the short wavelength (viz. high-m) modes suppression is achieved by the combined effect of poloidal MHD and ion diamagnetic flow with the constraint of a Doppler-like effect of the ion flow. This approximation has been employed primarily to keep the algebra manageable. A vacuum gap between plasma and the metallic wall is necessary, though its effect is weakened for sufficiently large m and reduced by the presence of the separatrix. Although highly simplified profiles for pressure, mass density and equilibrium rotation have been employed, all features measured experimentally and modelled numerically have been retrieved within the *exfernal* framework. These are: (i) the strong dependence of the EHO appearance on the $\boldsymbol{E} \times \boldsymbol{B}$ poloidal rotation letting low-n modes emerge, (ii) the independence of the growth rate upon the sign of the toroidal flow [17, 19, 44], (iii) the rotation frequency spacing of the toroidal harmonics close to the plasma toroidal rotation (if sufficiently large) at the pedestal top [10, 13] and (iv) the pedestal localised structure of the radial eigenfunction. Further work is required to extend the analysis of such phenomena with more realistic profiles in a beyond-MHD framework.

This work has been carried out within the framework of the EUROfusion Consortium and has received funding from the Euratom research and training programme 2014-2018 under grant agreement No 633053. The views and opinions expressed herein do not necessarily reflect those of the European Commission. This work was supported in part by the Swiss National Science Foundation.

* Electronic address: brunetti@ifp.cnr.it

[1] F. Wagner, Plasma Phys. Control. Fusion **49**, B1 (2007).
[2] A. W. Leonard, Phys. Plasmas **21**, 090501 (2014).
[3] C. M. Greenfield *et al.*, Phys. Rev. Lett. **86**, 4544 (2001).
[4] K. H. Burrell *et al.*, Plasma Phys. Control. Fusion **44**, A253 (2002).
[5] W. Suttrop *et al.*, Plasma Phys. Control. Fusion **45**, 1399 (2003).
[6] K. H. Burrell *et al.*, Phys. Plasmas **12**, 056121 (2005).
[7] X. Chen *et al.*, Nucl. Fusion **56**, 076011 (2016).
[8] K. H. Burrell *et al.*, Phys. Plasmas **8**, 2153 (2001).
[9] W. Suttrop *et al.*, Nucl. Fusion **45**, 721 (2005).
[10] E. R. Solano *et al.*, Phys. Rev. Lett. **104**, 185003 (2010).
[11] N. Oyama *et al.*, Nucl. Fusion **45**, 871 (2005).
[12] K. H. Burrell *et al.*, Nucl. Fusion **49**, 085024 (2009).
[13] L. J. Zheng *et al.*, Nucl. Fusion **53**, 063009 (2013).
[14] S. Y. Medvedev *et al.*, Plasma Phys. Control. Fusion **48**, 927 (2006).
[15] L. J. Zheng *et al.*, Phys. Plasmas **20**, 012501 (2013).
[16] G. Q. Dong *et al.*, Phys. Plasmas **24**, 112510 (2017).
[17] F. Liu *et al.*, Nucl. Fusion **55**, 113002 (2015).
[18] J. R. King *et al.*, Phys. Plasmas **24**, 055902 (2017).
[19] A. M. Garofalo *et al.*, Nucl. Fusion **51**, 083018 (2011).
[20] F. Liu *et al.*, Plasma Phys. Control. Fusion **60**, 014039 (2018).
[21] W. A. Cooper *et al.*, J. Plasma Phys. **81**, 515810605 (2015).
[22] W. A. Cooper *et al.*, Plasma Phys. Control. Fusion **58**, 064002 (2016).
[23] W. A. Cooper *et al.*, Phys. Plasmas **23**, 040701 (2016).
[24] A. Kleiner *et al.*, Nucl. Fusion **58**, 074001 (2018).
[25] D. Brunetti *et al.*, Nucl. Fusion **58**, 014002 (2018).
[26] D. Brunetti *et al.*, Plasma Phys. Control. Fusion **56**, 075025 (2014).
[27] R. D. Hazeltine and J. D. Meiss, *Plasma Confinement* (Addison-Wesley Publishing Company, Redwood City, 1992).
[28] A. M. Garofalo *et al.*, Phys. Plasmas **22**, 056116 (2015).
[29] Note that $v^\varphi = \boldsymbol{v} \cdot \boldsymbol{\nabla}\varphi$ has the dimensions of a frequency. Same argument applies to v^ϑ.
[30] C. Wahlberg *et al.*, Plasma Phys. Control. Fusion **55**, 105004 (2013).
[31] R. J. Hastie and T. C. Hender, Nucl. Fusion **28**, 585 (1988).
[32] C. G. Gimblett *et al.*, Phys. Plasmas **3**, 33691 (1996).
[33] W. Newcomb, Ann. Phys. **10**, 232 (1960).

[34] E. Frieman and M. Rotenberg, Rev. Mod. Phys. **32**, 898 (1960).
[35] B. Coppi *et al.*, Nucl. Fusion **6**, 101 (1966).
[36] A. B. Mikhailovskii, *Instabilities in a Confined Plasma* (IOP, Bristol, 1998).
[37] A. B. Mikhailovskii *et al.*, Nucl. Fusion **13**, 259 (1973).
[38] J. W. Haverkort and H. J. de Blank, Phys. Rev. E **86**, 016411 (2012).
[39] A. Bondeson *et al.*, Phys. Fluids **30**, 2167 (1987).
[40] A. H. Glasser *et al.*, Phys. Fluids **18**, 875 (1975).
[41] This is expected with $\omega^* \sim p_0' < 0$ and $\omega_\vartheta \sim -E_r > 0$ having the two frequencies comparable magnitude (see e.g. X. Chen *et al.*, Nucl. Fusion **57**, 086008 (2017).
[42] We assume that $\Omega(r_p) = \Omega(r_1)$ and $\rho_0(r_p) = \rho_0(r_1)$.
[43] H. J. de Blank and T. J. Schep, Phys. Fluids B **3**, 1136 (1991).
[44] K. H. Burrell *et al.*, Phys. Rev. Lett. **102**, 155003 (2009).
[45] T. M. Wilks *et al.*, Nucl. Fusion 58, 112002 (2018)